



1-Propanol as a co-guest of gas hydrates and its potential role in gas storage and CO₂ sequestration



Youngjun Lee^a, Seungmin Lee^b, Young Keun Jin^c, Yongwon Seo^{a,*}

^a School of Urban and Environmental Engineering, Ulsan National Institute of Science and Technology, Ulsan 689-798, Republic of Korea

^b Offshore Plant Resources R&D Center, Korea Institute of Industrial Technology, Busan 618-230, Republic of Korea

^c Division of Polar Earth-System Sciences, Korea Polar Research Institute, Incheon 406-840, Republic of Korea

HIGHLIGHTS

- We examine the enclathration of 1-propanol as a co-guest of gas hydrates.
- 1-Propanol forms cubic structure II hydrates with CH₄ and CO₂.
- 1-PrOH does not act as a notable hydrate promoter or an inhibitor for CH₄ hydrate.
- 1-PrOH functions as a significant thermodynamic hydrate inhibitor for CO₂ hydrate.

ARTICLE INFO

Article history:

Received 16 June 2014

Received in revised form 24 July 2014

Accepted 26 July 2014

Available online 5 August 2014

Keywords:

Gas hydrate

Gas storage

CO₂ sequestration

1-Propanol

Inhibitor

ABSTRACT

The inclusion of 1-propanol (1-PrOH) as a co-guest of gas hydrates in the presence of CH₄ and CO₂ and its potential role in gas storage and CO₂ sequestration were investigated focusing primarily on macroscopic hydrate phase equilibrium behavior and microscopic structural and cage filling characteristics. The powder X-ray diffraction (PXRD) patterns confirmed that both double CH₄ + 1-PrOH and double CO₂ + 1-PrOH hydrates are cubic structure II (sII) hydrates. 1-PrOH did not act as a remarkable thermodynamic hydrate promoter or inhibitor for CH₄ hydrate systems, though it did act as a significant thermodynamic hydrate inhibitor for CO₂ hydrate systems despite its participation as a co-guest in the hydrate lattices. The ¹³C NMR results revealed that 1-PrOH was found in the large 5¹²6⁴ cages of the sII hydrate along with CH₄ at lower 1-PrOH concentrations, and the chemical formulas for the double CH₄ + 1-PrOH hydrates were found to be 2.13 CH₄ · 0.53 1-PrOH · 17 H₂O for the 1-PrOH 1.0 mol% solution and 1.85 CH₄ · 0.75 1-PrOH · 17 H₂O for the 1-PrOH 5.6 mol% solution. The overall experimental results provide a better understanding of guest–host interaction, guest distributions, and structural transition in guest gas + 1-PrOH hydrates for the potential application of 1-PrOH in gas storage and CO₂ sequestration.

© 2014 Elsevier B.V. All rights reserved.

1. Introduction

Gas hydrates are non-stoichiometric crystal structures that can trap guest molecules in the well-defined host lattices built up from hydrogen-bonded water molecules. They have three distinct crystal types: structure I (sI), structure II (sII), and structure H (sH), which differ in sizes and shapes of the cages formed [1]. The chemistry of gas hydrates is an important issue in natural gas transportation because pipeline plugging due to gas hydrate formation can lead to serious safety problems and economic losses. The situation is even more serious in offshore oil and gas facilities where gas hydrates can block pipelines, which can result in major equipment

damage, significant loss of production, and possible leakage of oil and gas [2].

CO₂, which is mainly produced from the combustion of fossil fuels, can be stored in the ocean or underground [3–5]. For ocean or geological sequestration, CO₂ should be transported from emission sources to storage sites through pipelines. Because CO₂ forms gas hydrates under milder conditions than CH₄, it is also expected that CO₂ hydrate formation and subsequent pipeline plugging can be major issues during CO₂ transportation [1].

Massive efforts have been made to prevent hydrate plugging in pipelines [2]. For flow assurance, the method currently favored for industrial use is inhibitor injection. These inhibitors alter the conditions under which hydrates may form, preventing hydrates from forming in the pipeline. Alcohols are the most commonly used thermodynamic inhibitors. They are known to disrupt the water's

* Corresponding author. Tel.: +82 52 217 2821; fax: +82 52 217 2819.

E-mail address: ywseo@unist.ac.kr (Y. Seo).

hydrogen bonding network; thus, they inhibit the formation of gas hydrates without being trapped in the hydrate cages [2]. However, some researchers have recently reported that water-soluble alcohols, such as ethanol, propanols, and tert-butanol, form sII hydrates and act as guests of the hydrate structures in the presence of hydrophobic gases, such as CH₄ and CO₂ [6–18]. Furthermore, even methanol, the most widely used thermodynamic hydrate inhibitor, has recently been found to be able to be incorporated in the hydrate cages as a guest [19].

1-Propanol (1-PrOH), a secondary alcohol, was reported to form simple hydrates of cubic structure at temperatures much lower than the freezing point of water, but it also forms double 1-PrOH hydrates under the pressure of a help gas such as CH₄ [11,12,16–18,20]. The Raman spectrum and powder X-ray diffraction (PXRD) pattern of the double CH₄ + 1-PrOH hydrates indicated the formation of sII hydrates and the molecular dynamic simulations and thermodynamic modeling predicted the occupation of 1-PrOH in the large cages of sII hydrates under the pressurization of CH₄ [11,12,18]. However, the guest distribution and cage occupancy of each guest in sII double CH₄ + 1-PrOH hydrates have not yet been clearly revealed. In particular, the double hydrates of CO₂ + 1-PrOH have not yet been explored.

The enclathration of alcohols as guests in hydrate cages and their thermodynamic effects on hydrate equilibrium conditions are very crucial factors in flow assurance. This study examines the unique pattern and distribution of guest molecules in double 1-PrOH hydrates formed with either CH₄ or CO₂ as a help gas, focusing primarily on macroscopic hydrate equilibrium behaviors and microscopic analytical methods, such as ¹³C NMR spectroscopy and PXRD. The three-phase hydrate equilibria (gas hydrate (H)–liquid water (L_w)–vapor (V)) for the ternary CH₄ + 1-PrOH + water and CO₂ + 1-PrOH + water mixtures at three different 1-PrOH concentrations (1.0, 5.6, and 10.0 mol%) were measured to examine the effect of 1-PrOH enclathration on the thermodynamic stability of the double hydrates. The crystal structures of both double CH₄ + 1-PrOH and double CO₂ + 1-PrOH hydrates were identified via PXRD. Accurate information on the guest distribution and cage occupancy of each guest in the CH₄ + 1-PrOH hydrates was examined via ¹³C NMR spectroscopy.

2. Experimental

2.1. Materials

The CH₄ and CO₂ gases, which had stated purity values of 99.95% and 99.99%, respectively, were provided by PSG Gas Co. (Republic of Korea). 1-PrOH used in this study had a purity of 99.5%; it was purchased from Sigma–Aldrich (USA). Double distilled and deionized water was used. No further purification was carried out on any of the materials used.

2.2. Phase equilibrium measurements

An equilibrium cell with two sapphire windows was constructed for the hydrate phase equilibrium measurements. The cell, with an internal volume of approximately 200 cm³, was made from 316 stainless steel and was immersed in the water bath. The windows were located at the front and the back of the cell in order to allow visual observation of phase transitions inside. An impeller type stirrer was used to agitate the cell content vigorously. The thermocouple used for temperature measurement has an accuracy of ±0.1 K for full ranges. The pressure transducer (S-10, 0–10.0 MPa, Wika, Germany) has an accuracy of ±0.25%, which was calibrated using a Heise Bourdon tube pressure gauge (CMM-137219, 0–10.0 MPa) with a maximum error of ±0.01 MPa in the full range.

An isochoric pressure search method with step heating was adopted for the H–L_w–V equilibrium measurement. The equilibrium cell was initially charged with approximately 90 cm³ of 1-PrOH solution, and CH₄ or CO₂ was added until the target pressure was reached. Next, in order to nucleate hydrate crystals the cell temperature was decreased at a cooling rate of 1.0 K steps with a 60 min interval. A sudden pressure drop confirmed the formation of hydrates. This reduction in pressure was caused by the enclathration of gas molecules in the hydrate phase. After the completion of gas hydrate formation, the temperature was raised in 0.1 K steps with a 90 min interval, leading to an increase in cell pressure with corresponding hydrate dissociation. The H–L_w–V equilibrium point for each pressure condition could be determined by the intersection point between the hydrate dissociation line and the thermal expansion line in the pressure–temperature trace for formation and dissociation of CH₄ (or CO₂) + 1-PrOH hydrates. A schematic diagram of the experimental apparatus and a more detailed description of the experimental procedure were given in previous papers [21–23].

2.3. PXRD and ¹³C NMR analyses

A Rigaku Geigerflex diffractometer (D/Max-RB) with graphite-monochromatized Cu Kα1 radiation (λ = 1.5406 Å) was used to identify the crystal structures of the double CH₄ + 1-PrOH and CO₂ + 1-PrOH hydrates. Prior to taking PXRD measurements, the gas hydrate samples were prepared in the equilibrium cell under high pressure and then were transferred to a liquid nitrogen vessel where they were finely powdered by grinding. The PXRD data were collected by step mode with a fixed time of 3 s and a step size of 0.02° for 2θ = 10–60° at 133.15 K. Analysis of the observed patterns was carried out using the Checkcell program.

The crystal structure and guest distributions of the double CH₄ + 1-PrOH hydrates were investigated using a Bruker 400 MHz solid-state NMR spectrometer (Bruker, Germany). The prepared hydrate samples were loaded in a zirconia rotor with 4 mm o.d. before being placed into the variable-temperature (VT) probe. All ¹³C NMR spectra were recorded at a Larmor frequency of 100.6 MHz with magic angle spinning (MAS) between 2 and 4 kHz at 243 K and atmospheric pressure. A pulse length of 2 μs and a pulse repetition delay of 10 s under proton decoupling were employed when a radio frequency field strength of 50 kHz corresponding to 5 μs 90° pulses was used. A chemical shift of 38.3 ppm at 300 K, corresponding to the downfield carbon resonance peak of adamantane, was used as an external chemical shift reference. A more detailed explanation of the PXRD and ¹³C NMR analysis was provided in previous papers [24,25].

3. Results and discussion

3.1. PXRD

It has already been established that both pure CH₄ and pure CO₂ form sI hydrates [1]. However, the large molecular size of 1-PrOH means that its inclusion in hydrate lattices with pressurization of CH₄ or CO₂ can cause a structural transition of the sI hydrates to sII double hydrates [11,12]. In this study, the crystal structure of double 1-PrOH hydrates with CH₄ and CO₂ was determined using PXRD measurements. Fig. 1 presents the PXRD patterns of both the double CH₄ + 1-PrOH (5.6 mol%) hydrate and the double CO₂ + 1-PrOH (5.6 mol%) hydrate measured at 133.15 K. The double CH₄ + 1-PrOH hydrate was found to be a cubic (*Fd3m*) sII structure with a unit cell parameter of 17.29 Å, which is in good agreement with the value reported by Ohmura et al. [14]. The double CO₂ + 1-PrOH hydrate was also identified as a cubic (*Fd3m*) sII

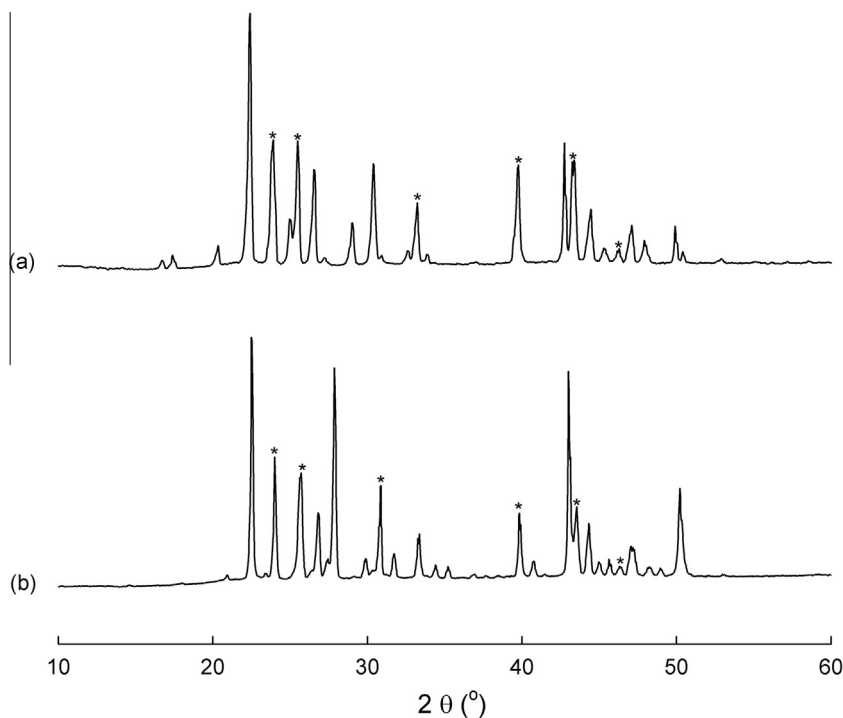


Fig. 1. (a) PXRD pattern of the double $\text{CH}_4 + 1\text{-PrOH}$ (5.6 mol%) hydrate (8.0 MPa and 278.15 K) and (b) PXRD pattern of the double $\text{CO}_2 + 1\text{-PrOH}$ (5.6 mol%) hydrate (3.7 MPa and 275.15 K). Asterisks indicate the hexagonal ice (Ih) phase.

structure with a 17.32 Å lattice constant. For the $\text{CO}_2 + 1\text{-PrOH}$ hydrate, the confirmation of sII hydrate formation and the characterization via PXRD were first reported in this study. The PXRD results clearly demonstrate that the enclathration of 1-PrOH molecules in the hydrate cages alters the sI pure CH_4 and CO_2 hydrates to the sII double hydrates.

3.2. Stability conditions

Fig. 2 and Table 1 present the H–L_W–V equilibrium data of the $\text{CH}_4 + 1\text{-PrOH}$ hydrates at three different 1-PrOH concentrations (1.0, 5.6, and 10.0 mol%) with the relevant reference data [11,16,26]. Although a substantial thermodynamic promotion effect was predicted from the inclusion of 1-PrOH molecules in the hydrate cages, this was not observed, as shown in Fig. 2. In general, thermodynamic hydrate promoters such as 1,4-dioxane and tetrahydrofuran occupy the large $5^{12}6^4$ cages of sII hydrates and stabilize the hydrate structure, resulting in a remarkable thermodynamic promotion represented by an equilibrium temperature increase and equilibrium pressure reduction [27,28]. However, as seen in Fig. 2, at low pressure ranges a slight thermodynamic promotion due to the addition of 1-PrOH was observed and the extent of the thermodynamic promotion was dependent on the 1-PrOH concentrations, which is generally observed in the other promoter added systems [27,28]. The promotion effect increased up to 5.6 mol%, which is a stoichiometric concentration of the sII hydrates, and at 1-PrOH 10.0 mol%, it is slightly decreased due to the presence of excess 1-PrOH molecules that are not enclathrated in the hydrate cages and thus may function as inhibitors. At high pressure ranges, a slight thermodynamic inhibition was observed for all 1-PrOH concentrations despite the enclathration of 1-PrOH molecules in the hydrate cages.

The hydrate phase equilibria of the $\text{CO}_2 + 1\text{-PrOH} + \text{water}$ systems at three different 1-PrOH concentrations (1.0, 5.6, and 10.0 mol%) are shown in Fig. 3 with the relevant reference data [26,29] and listed in Table 2. The effect of 1-PrOH concentrations

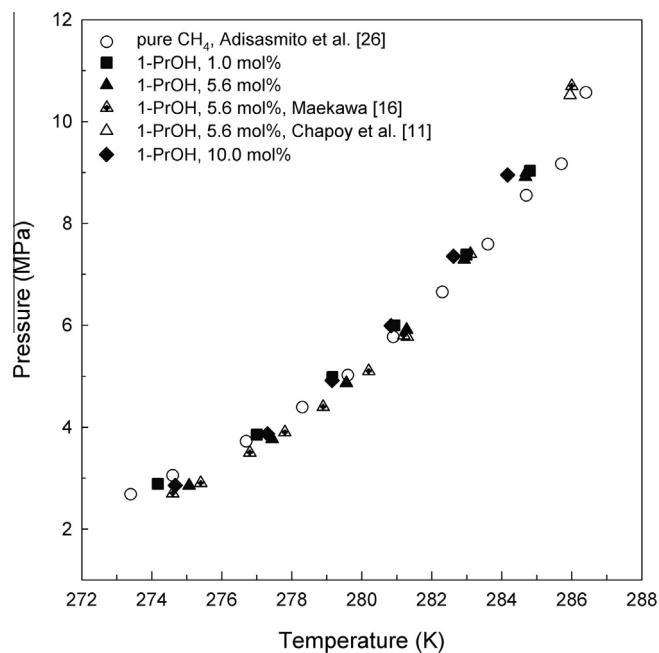


Fig. 2. Hydrate phase equilibria of the $\text{CH}_4 + 1\text{-PrOH} + \text{water}$ mixtures.

on the hydrate equilibrium line shift was more significant for the $\text{CO}_2 + 1\text{-PrOH} + \text{water}$ systems than that for the $\text{CH}_4 + 1\text{-PrOH} + \text{water}$ systems. Thermodynamic inhibition increased with an increase in 1-PrOH concentrations as is commonly observed in the conventional inhibitor-added systems [2]. Conventional thermodynamic inhibitors, such as ethylene glycol and sodium chloride, are not captured in the hydrate lattices. Instead, they disrupt the water–water hydrogen bonding network and, accordingly, make it difficult to convert all water to hydrate, resulting in a shift of the equilibrium line to the inhibition region [2].

Table 1
Hydrate phase equilibrium data for the CH₄ + 1-PrOH + water systems.

1.0 mol%		5.6 mol%		10.0 mol%	
T (K)	P (MPa)	T (K)	P (MPa)	T (K)	P (MPa)
274.2	2.89	275.1	2.85	274.7	2.86
277.0	3.85	277.4	3.77	277.3	3.87
279.2	4.98	279.6	4.87	279.2	4.92
280.9	5.99	281.3	5.91	280.8	5.99
283.0	7.39	282.9	7.29	282.6	7.35
284.8	9.04	284.7	8.92	284.2	8.95

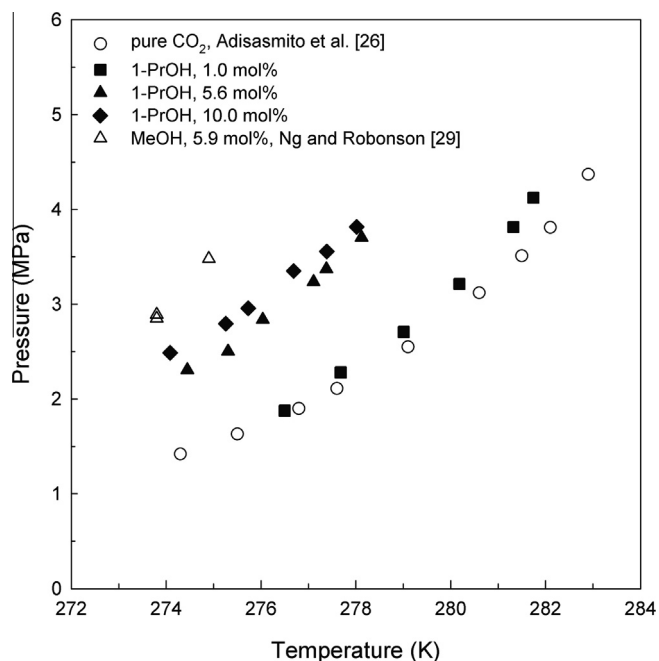


Fig. 3. Hydrate phase equilibria of the CO₂ + 1-PrOH + water mixtures.

Table 2
Hydrate phase equilibrium data for the CO₂ + 1-PrOH + water systems.

1.0 mol%		5.6 mol%		10.0 mol%	
T (K)	P (MPa)	T (K)	P (MPa)	T (K)	P (MPa)
276.5	1.88	274.4	2.31	274.1	2.49
277.7	2.28	275.3	2.50	275.3	2.79
279.0	2.71	276.0	2.84	275.7	2.96
280.2	3.21	277.1	3.24	276.7	3.35
281.3	3.81	277.4	3.37	277.4	3.56
281.7	4.12	278.1	3.70	278.0	3.82

Although 1-PrOH showed thermodynamic inhibition for the CO₂ hydrate, it should be noted that 1-PrOH was found to be enclathrated in the hydrate lattices, leading to the structural transition to the sII hydrate as revealed by PXRD. The enclathration of large guest molecules in the hydrate cages is generally expected to cause thermodynamic promotion, but recent investigations have reported that thermodynamic inhibition can also occur despite the inclusion of these molecules in the hydrate lattices [9,15]. In CO₂ + 1-PrOH hydrates, the fact that 1-PrOH is included in the hydrate lattices at the same time as it appears to act as a thermodynamic inhibitor can be attributed to the stronger hydrogen bonding between guest and host molecules and the lower cage occupancy of 1-PrOH molecules in the large 5¹²6⁴ hydrate cages. As indicated by the molecular dynamic simulations of Alavi et al. [30], the probability of hydrogen bonding between guest alcohol and host water in CO₂ + alcohol hydrates is more significant than

that in CH₄ + alcohol hydrates. The strong hydrogen bonding between guest 1-PrOH and host water disrupts the hydrogen bonding network of the host water molecules and as a result, weakens the stability of the hydrate structure. Furthermore, molecular dynamic simulations and microscopic analyses indicate that the cage occupancy of alcohol molecules in the CO₂ + alcohol hydrates is lower than that in the CH₄ + alcohol hydrates [8,9,30]. Accordingly, the lower cage occupancy of 1-PrOH molecules in the large 5¹²6⁴ cages of the sII hydrates also resulted in less stabilization of the hydrate structure.

3.3. ¹³C NMR and cage occupancy

¹³C MAS NMR spectroscopy is a powerful method to identify the structure type of gas hydrates and to quantify the compositions of each guest in the hydrate phase [31]. The cage-dependent ¹³C NMR chemical shift for the CH₄ molecules captured in the hydrate phase can function as an effective and convenient indicator of the structure types of the formed gas hydrates. Fig. 4(a) presents a stacked plot of the ¹³C MAS NMR spectra of the pure CH₄ hydrate, liquid 1-PrOH, double CH₄ + 1-PrOH (1.0 mol%) hydrate, and double CH₄ + 1-PrOH (5.6 mol%) hydrate. The pure CH₄ hydrate showed two resonance peaks at −4.3 and −6.6 ppm. The peak at −4.3 ppm can be assigned to the CH₄ molecules captured in the small 5¹² cages of the sI hydrate, and the peak at −6.6 ppm can be assigned to the CH₄ molecules enclathrated in the large 5¹²6² cages of the sI hydrate. The liquid 1-PrOH exhibited three resonance peaks with the same intensity at 63.6, 25.9, and 10.3 ppm. In the CH₄ + 1-PrOH (5.6 mol%) hydrate, the resonance peak at −4.5 ppm denotes the CH₄ molecules captured in the small 5¹² cages of the sII hydrate. Three large resonance peaks, which can be assigned to the unclathrated liquid 1-PrOH molecules, appeared at 63.6, 25.9, and 10.3 ppm, whereas three small resonance peaks, which can be assigned to the 1-PrOH molecules enclathrated in the large 5¹²6⁴ cages of the sII hydrates, were detected at 64.1, 25.3, and 9.8 ppm.

In the CH₄ + 1-PrOH (1.0 mol%) hydrate, the resonance peaks for the 1-PrOH molecules enclathrated in the large 5¹²6⁴ cages of the sII hydrate appeared again at 64.1, 25.3, and 9.8 ppm and the resonance peaks for the unreacted liquid 1-PrOH molecules were present in reduced size at 63.6, 25.9, and 10.3 ppm. There exist significant resonance peaks from both the CH₄ molecules of the sI hydrate and the CH₄ molecules of the sII hydrate. CH₄ molecules enclathrated in the small 5¹² and large 5¹²6² cages of the sI hydrate are responsible for resonance peaks at −4.3 and −6.6 ppm, respectively, whereas the CH₄ molecules captured in the small 5¹² and large 5¹²6⁴ cages of the sII hydrate have resonance peaks at −4.5 and −8.2 ppm, respectively. The coexistence of both sI and sII hydrates is frequently seen in the systems containing water soluble sII hydrate formers at concentrations lower than the stoichiometric level because the remaining water phase, which was not involved in the sII hydrate formation, can be used for additional pure CH₄ hydrate formation [32,33]. As is clearly shown in Fig. 4(b), the resonance peaks (−4.3 and −4.5 ppm) from CH₄ molecules captured in the small cages of each structure were located too close together because both sI and sII structures have the common 5¹² cages with almost the same dimension. However, the resonance peaks (−6.6 and −8.2 ppm) from CH₄ molecules captured in the large cages of each structure were distinctive because there is a big difference between the size and shape of the large cage of the sI hydrate and the large cage of the sII hydrate [1]. Therefore, the chemical shift from the CH₄ molecules captured in the large cages of each structure can be used as an effective indicator for determining the structure of the gas hydrates formed.

As seen in Fig. 4(a), in the CH₄ + 1-PrOH (5.6 mol%) hydrate, the large 5¹²6⁴ cages were occupied only by 1-PrOH molecules, while

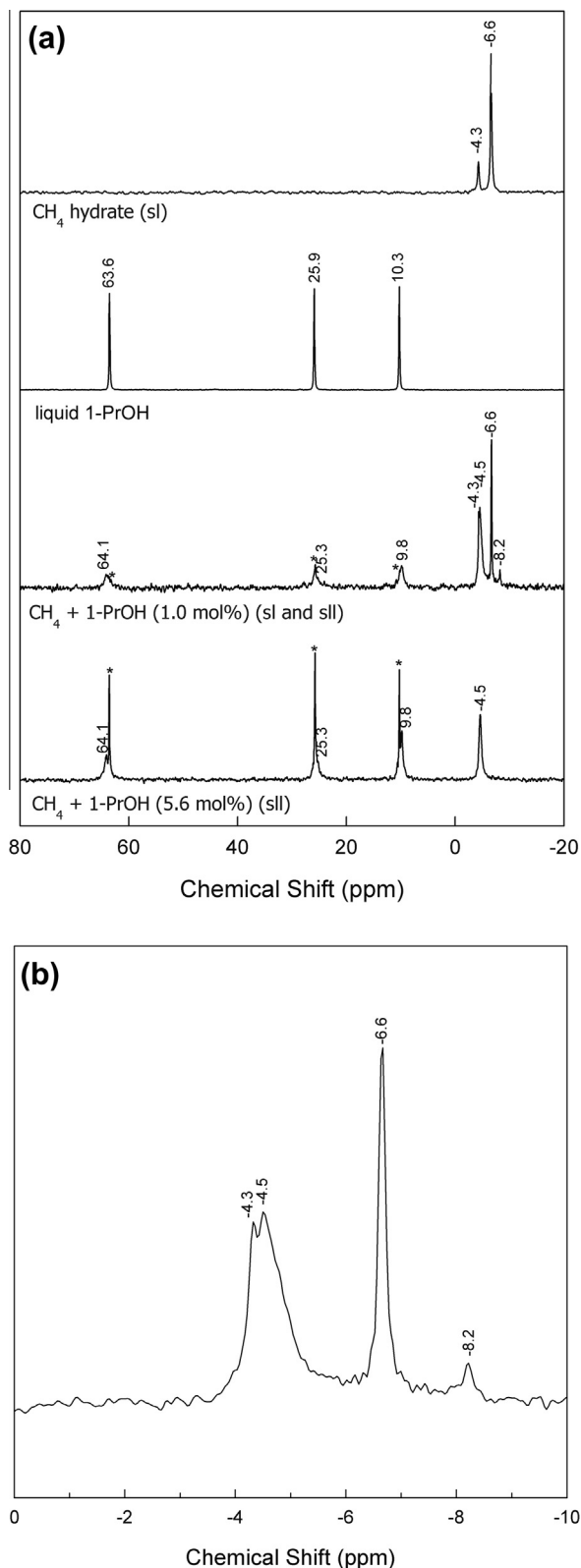


Fig. 4. (a) ¹³C NMR spectra of the pure CH₄ hydrate (8.0 MPa and 275.15 K), liquid 1-PrOH, double CH₄ + 1-PrOH (1.0 mol%) hydrate (8.0 MPa and 278.15 K), and double CH₄ + 1-PrOH (5.6 mol%) hydrate (8.0 MPa and 278.15 K) and (b) ¹³C NMR spectrum of the double CH₄ + 1-PrOH (1.0 mol%) hydrate in the upfield region. Asterisks indicate the resonance peaks from the unclathrated liquid 1-PrOH.

in the CH₄ + 1-PrOH (1.0 mol%) hydrate, the large 5¹²6⁴ cages were shared by both 1-PrOH and CH₄ molecules. Guest distributions and cage occupancy of each guest in the double 1-PrOH hydrates can be

affected by 1-PrOH concentrations. The accurate cage occupancy of each guest in the double CH₄ + 1-PrOH hydrates can be determined by combining the following statistical thermodynamic expressions with the relative integrated resonance peak areas of each guest [34]:

$$\Delta\mu_w^0 = -\frac{RT}{17} [\ln(1 - \theta_{l,1-PrOH} - \theta_{l,CH_4}) + 2 \ln(1 - \theta_{s,CH_4})]$$

where $\Delta\mu_w^0$ is the chemical potential of the empty lattice relative to the ice, θ_s is the fractional occupancy of the small cages, and θ_l is the fractional occupancies of the large cages. For sll hydrates, a $\Delta\mu_w^0$ value of 883.8 J/mol was used. More detailed descriptions of cage occupancy calculation have been given in previous papers [15,23]. The calculated cage occupancies of each guest are shown in Fig. 5 and listed in Table 3. The cage occupancy of CH₄ in the small 5¹² cages was hardly affected by the 1-PrOH concentrations. However, the cage occupancy of 1-PrOH in the large 5¹²6⁴ cages was significantly increased with an increase in the 1-PrOH concentration. The lower cage occupancy of 1-PrOH in the large 5¹²6⁴ cages at 1.0 mol% resulted in the additional occupation of CH₄ in the large 5¹²6⁴ cages. The CH₄ + 1-PrOH hydrates demonstrated the relatively lower cage occupancy of alcohols in the large 5¹²6⁴ cages of the sll hydrate for all concentration ranges when compared with the CH₄ + 2-PrOH hydrates [15]. The lower cage occupancy of 1-PrOH in the large cages of the CH₄ + 1-PrOH hydrates lead to lower thermodynamic promotion compared with the CH₄ + 2-PrOH hydrates. The cage occupancies of each guest in the CH₄ + 1-PrOH hydrates provide the chemical formula of 2.13 CH₄ · 0.53 1-PrOH · 17 H₂O

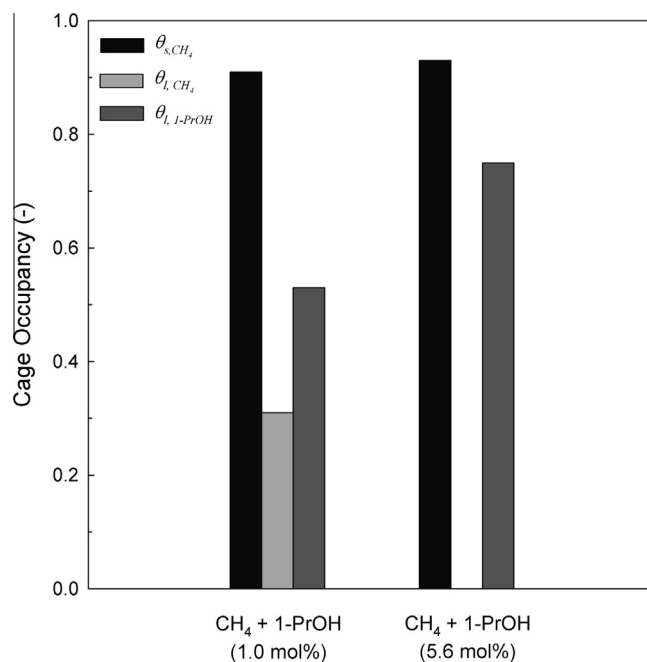


Fig. 5. Cage occupancies of the CH₄ and 1-PrOH molecules in the double CH₄ + 1-PrOH hydrates at two different 1-PrOH concentrations of 1.0 and 5.6 mol%.

Table 3
Cage occupancies of the double CH₄ + 1-PrOH hydrates.

System	CH ₄		2-PrOH
	θ_{s,CH_4}	θ_{l,CH_4}	$\theta_{l,1-PrOH}$
CH ₄ + 1-PrOH (1.0 mol%)	0.91	0.31	0.53
CH ₄ + 1-PrOH (5.6 mol%)	0.93	0	0.75

for the 1-PrOH 1.0 mol% solution and 1.85 CH₄ · 0.75 1-PrOH · 17 H₂O for the 1-PrOH 5.6 mol% solution. The ¹³C MAS NMR results indicate that the cage filling characteristics and the guest distributions in the CH₄ + 1-PrOH hydrates are closely related to the 1-PrOH concentrations.

3.4. Overall remarks

Because 1-PrOH showed slight thermodynamic promotion in low-pressure regions and slight thermodynamic inhibition in high-pressure regions in the presence of CH₄ as a help gas, 1-PrOH cannot be expected to be useful as a thermodynamic hydrate promoter which can reduce hydrate formation pressure at a specified temperature for natural gas storage or as a thermodynamic inhibitor which can prevent pipeline plugging problems in oil and gas production facilities. On the contrary, 1-PrOH demonstrated significant thermodynamic inhibition in the presence of CO₂ as a help gas; thus, it is a good candidate for a thermodynamic hydrate inhibitor which can prevent CO₂ hydrate formation in pipelines for the transportation of CO₂ to sequestration sites. However, it should be noted that 1-PrOH can be enclathrated as a co-guest in hydrate lattices; thus, it forms the sII double hydrates with CH₄ and CO₂.

4. Conclusion

In this study, the stability conditions, crystal structure, and guest distribution of double 1-PrOH hydrates with CH₄ and CO₂ were determined through macroscopic hydrate phase equilibrium measurements and microscopic analytical methods such as ¹³C NMR spectroscopy and PXRD. The inclusion of 1-PrOH molecules in the hydrate lattices and the subsequent structural transition to the sII hydrate were confirmed from the PXRD patterns and the ¹³C NMR spectra. For the CH₄ + 1-PrOH hydrates, the inclusion of 1-PrOH molecules in the large 5¹²6⁴ cages of the double sII hydrates did not lead to remarkable thermodynamic promotion. Due to the lower cage occupancy of 1-PrOH molecules in the hydrate cages and the stronger hydrogen bonding between guest and host molecules, the CO₂ + 1-PrOH hydrates exhibited more significant thermodynamic inhibition. From the cage dependent ¹³C NMR spectra, it was found that both CH₄ and 1-PrOH molecules occupied the large 5¹²6⁴ cages of the sII hydrate formed from the PrOH 1.0 mol% solution while only 1-PrOH molecules occupied the large 5¹²6⁴ cages of the sII hydrate formed from the PrOH 5.6 mol% solution. The data gained from this experiment are expected to improve knowledge of structural transition, guest distributions, and cage filling characteristics of guest gas + 1-PrOH hydrates for the potential use of 1-PrOH in industrial applications.

Acknowledgements

This research was supported by the Korea Polar Research Institute (KOPRI, Grant No. PE14061) and also by the Basic Science Research Program through the National Research Foundation of Korea (NRF) funded by the Ministry of Education (2012R1A1B6002494).

References

- [1] E.D. Sloan, C.A. Koh, *Clathrate Hydrates of Natural Gases*, third ed., CRC Press, Boca Raton, 2008.
- [2] C.A. Koh, E.D. Sloan, A. Sum, *Natural Gas Hydrates in Flow Assurance*, Gulf Professional Publishing, Burlington, 2011.
- [3] IPCC special report on carbon dioxide capture and storage, <<http://www.ipcc.ch>>.
- [4] H. Lee, Y. Seo, Y.T. Seo, I.L. Moudrakovski, J.A. Ripmeester, Recovering methane from solid methane hydrate with carbon dioxide, *Angew. Chem. Int. Ed.* 42 (2003) 5048–5051.

- [5] P. Babu, R. Kumar, P. Linga, Pre-combustion capture of carbon dioxide in a fixed bed reactor using the clathrate hydrate process, *Energy* 50 (2013) 364–373.
- [6] K. Yasuda, S. Takeya, M. Sakashita, H. Yamawaki, R. Ohmura, Binary ethanol–methane clathrate hydrate formation in the system CH₄–C₂H₅OH–H₂O: confirmation of structure II hydrate formation, *J. Phys. Chem. C* 113 (2009) 12598–12601.
- [7] R. Anderson, A. Chapoy, H. Haghghi, B. Tohidi, Binary ethanol–methane clathrate hydrate formation in the system CH₄–C₂H₅OH–H₂O: phase equilibria and compositional analyses, *J. Phys. Chem. C* 113 (2009) 12602–12607.
- [8] T. Makiya, T. Murakami, S. Takeya, A.K. Sum, S. Alavi, R. Ohmura, Synthesis and characterization of clathrate hydrates containing carbon dioxide and ethanol, *Phys. Chem. Chem. Phys.* 12 (2010) 9927–9932.
- [9] J.W. Lee, S.P. Kang, Spectroscopic identification on cage occupancies of binary gas hydrates in the presence of ethanol, *J. Phys. Chem. B* 116 (2012) 332–335.
- [10] Y. Park, M. Cha, W. Shin, H. Lee, J.A. Ripmeester, Spectroscopic observation of critical guest concentration appearing in tert-butyl alcohol clathrate hydrate, *J. Phys. Chem. B* 112 (2008) 8443–8446.
- [11] A. Chapoy, R. Anderson, H. Haghghi, T. Edward, B. Tohidi, Can n-propanol form hydrate?, *Ind. Eng. Chem. Res.* 47 (2008) 1689–1694.
- [12] K. Yasuda, S. Takeya, M. Sakashita, H. Yamawaki, R. Ohmura, Characterization of the clathrate hydrate formed with methane and propan-1-ol, *Ind. Eng. Chem. Res.* 48 (2009) 9335–9337.
- [13] K. Østergaard, B. Tohidi, R. Anderson, A.C. Todd, A. Danesh, Can 2-propanol form clathrate hydrates?, *Ind. Eng. Chem. Res.* 41 (2002) 2064–2068.
- [14] R. Ohmura, S. Takeya, T. Uchida, T. Ebinuma, Clathrate hydrate formed with methane and 2-propanol: confirmation of structure II hydrate formation, *Ind. Eng. Chem. Res.* 43 (2004) 4964–4966.
- [15] Y. Lee, S. Lee, S. Park, Y. Kim, J.W. Lee, Y. Seo, 2-propanol as a co-guest of structure II hydrates in the presence of help gases, *J. Phys. Chem. B* 117 (2013) 2449–2455.
- [16] T. Maekawa, Equilibrium conditions for clathrate hydrates formed from methane and aqueous propanol solutions, *Fluid Phase Equilib.* 267 (2008) 1–5.
- [17] F.V. Zhurko, A.Y. Manakov, V. Kosyakov, Formation of gas hydrates in the systems methane–water–ROH (ROH = ethanol, n-propanol, i-propanol, i-butanol), *Chem. Eng. Sci.* 65 (2010) 900–905.
- [18] S. Alavi, S. Takeya, R. Ohmura, T.K. Woo, J.A. Ripmeester, Hydrogen-bonding alcohol–water interactions in binary ethanol, 1-propanol, and 2-propanol + methane structure II clathrate hydrates, *J. Chem. Phys.* 133 (2010) 074505.
- [19] K. Shin, K.A. Udachin, I.L. Moudrakovski, D.M. Leek, S. Alavi, C.I. Ratcliffe, J.A. Ripmeester, Methanol incorporation in clathrate hydrates and the implications for oil and gas pipeline flow assurance and icy planetary bodies, *Proc. Natl. Acad. Sci. U.S.A.* 110 (2013) 8439–8442.
- [20] A.Yu. Manakov, L.S. Aladko, A.G. Ogienko, A.I. Ancharov, Hydrate formation in the system n-propanol–water, *J. Therm. Anal. Calorim.* 111 (2013) 885–890.
- [21] Y. Seo, H. Lee, Phase behavior and structure identification of the mixed chlorinated hydrocarbon clathrate hydrates, *J. Phys. Chem. B* 106 (2002) 9668–9673.
- [22] I. Cha, S. Lee, J.D. Lee, G.W. Lee, Y. Seo, Separation of SF₆ from gas mixtures using gas hydrate formation, *Environ. Sci. Technol.* 44 (2010) 6117–6122.
- [23] S. Lee, Y. Seo, Experimental measurement and thermodynamic modeling of the mixed CH₄ + C₃H₈ clathrate hydrate equilibria in silica gel pores: effect of pore size and salinity, *Langmuir* 26 (2010) 9742–9748.
- [24] S. Lee, S. Park, Y. Lee, J. Lee, H. Lee, Y. Seo, Guest gas enclathration in semiclathrates of tetra-n-butyl ammonium bromide: stability condition and spectroscopic analysis, *Langmuir* 27 (2011) 10597–10603.
- [25] S. Lee, Y. Lee, S. Park, Y. Seo, Structural transformation of isopropylamine semiclathrate hydrates in the presence of methane as a co-guest, *J. Phys. Chem. B* 116 (2012) 13476–13480.
- [26] S. Adisasmito, R.J. Frank, E.D. Sloan, Hydrates of carbon dioxide and methane mixtures, *Chem. Eng. Data* 36 (1991) 68–71.
- [27] M.D. Jager, R.M. de Deugd, C.J. Peters, J. de Swaan Arons, E.D. Sloan, Experimental determination and modeling of structure II hydrates in mixtures of methane + water + 1,4-dioxane, *Fluid Phase Equilib.* 165 (1999) 209–223.
- [28] Y. Seo, S.P. Kang, S. Lee, H. Lee, Experimental measurements of hydrate phase equilibria for carbon dioxide in the presence of THF, propylene oxide, and 1,4-dioxane, *J. Chem. Eng. Data* 53 (2008) 2833–2837.
- [29] H.J. Ng, D.B. Robinson, Hydrate formation in systems containing methane, ethane, propane, carbon dioxide or hydrogen sulfide in the presence of methanol, *Fluid Phase Equilib.* 21 (1985) 145–155.
- [30] S. Alavi, R. Ohmura, J.A. Ripmeester, A molecular dynamic study of ethanol–water hydrogen bonding in binary structure I clathrate hydrate with CO₂, *J. Chem. Phys.* 134 (2011) 054702.
- [31] J.A. Ripmeester, C.I. Ratcliffe, On the contributions of NMR spectroscopy to clathrate science, *J. Struct. Chem.* 40 (1999) 654–662.
- [32] D.Y. Kim, J. Park, J.W. Lee, J.A. Ripmeester, H. Lee, Critical guest concentration and complete tuning pattern appearing in the binary clathrate hydrates, *J. Am. Chem. Soc.* 128 (2006) 15360–15361.
- [33] Y. Seo, J.W. Lee, R. Kumar, I.L. Moudrakovski, H. Lee, J.A. Ripmeester, Tuning the composition of guest molecules in clathrate hydrates: NMR identification and its significance to gas storage, *Chem. Asian J.* 4 (2009) 1266–1274.
- [34] J.H. van der Waals, J.C. Platteeuw, Clathrate solutions, *Adv. Chem. Phys.* 2 (1959) 1–58.